J. Applied Membrane Science & Technology, Vol. 22, No. 2 December 2018, 85–99

Verification of a Combined Fouling Model to Predict Flux Decline during Ultrafiltration of Organic Solutes

I. N. H. M. Amin[a*] & A. W. Mohammad[b]

[a]Section of Chemical Engineering Technology, Universiti Kuala Lumpur Malaysian Institute of Chemical & Bioengineering Technology, Lot 1988 Kaw. Perindustrian Bdr. Vendor, Taboh Naning, 78000 Alor Gajah, Melaka, Malaysia
[b]Department of Chemical and Process Engineering, Faculty of Engineering & Built Environment, Universiti Kebangsaan Malaysia, 43600 Bangi, Selangor, Malaysia

Submitted: 16/9/2018. Revised edition: 21/10/2018. Accepted: 22/10/2018. Available online: 21/11/2018

ABSTRACT

Studies were conducted to investigate the blocking mechanism and flux decline behavior while treating organic solutes contained in glycerin-water solutions (triglycerides, TG and fatty acid, FA). Two ultrafiltration membranes were tested, polyethersulphone (PES 25 kDa) and polyvinylidenfluoride (PVDF 30 kDa) membranes. Influence of TG and its combination (TG–FA mixtures) as foulant models, pH of feed solutions (3–10) and membrane surface chemistry were investigated. Combined blocking model was applied and the fitting were discriminate that the flux decline of PES membrane was dominated by pore blockage at the early stage and later by cake resistance during the entire filtration time. However, for PVDF membrane, cake formation mechanism was acknowledged as the major contributor to the fouling mechanism for all the parameters tested. On the other hand, the model predicts there are two stages of filtration appeared to occur, involving pore blockage at the early stage followed by cake formation.

Keywords: Blocking mechanism, fatty acid, flux decline, hydrophobic solute, sweetwater

1.0 INTRODUCTION

Glycerin, also called as glycerol, is one of most versatile chemicals which has variety of uses in pharmaceutical, cosmetic, food, tobacco, paint, automotive, leather and textile industries [1]. Glycerin is generally produced from hydrolysis and saponification reaction in oleochemical plants as the major byproduct. In addition, glycerin is now greatly generated from transesterification of fats or oils in biodiesel plants. However, glycerin-rich solutions produced in oleochemical and biodiesel plants contain various impurities depending on the synthesis process and the type of oil or fat processed. For example, sweetwater or glycerin-rich solution from hydrolysis reaction contains a mixture of glycerin, water and impurities such as free fatty acid, unreacted mono-, di-, and triglycerides, inorganic salts and variety of matter organic non-glycerol (MONG) [1-3].

The need for pure glycerin from hydrolysis process requires removal of impurities as well as water from crude glycerin [4]. In the existing industry practice, sweetwater with 15 wt % of glycerin will be concentrated to crude glycerol (80 wt% purity) after chemical pretreatment and evaporation. The crude glycerol is then further concentrated to pure glycerol

* Corresponding to: I. N. H. M. Amin (email: nurulhasyimah@unikl.edu.my)

with a purity exceeding 99 wt% of glycerol using distillation units [4].

Since membrane technology has been widely utilized in other areas, it is interested in further exploring the application of membranes in glycerin purification. Ultrafiltration (UF) could be an alternative to the chemical pretreatment and wastewater treatment [5, 6]. However, one of the main barrier in implementing UF would be due to fouling [7].

Essentially, a classical variation of permeate flux with time is an initial and rapid reduction followed by a gradual decline and, consequently, severe membrane fouling. It has been reported in the literature that this might be due to solute adsorption inside the membrane, blockage of pores, concentration polarisation or solute deposition on the membrane surface to form a cake layer [8]. It has been reported that pore blockage and cake formation occurs simultaneously. Pan *et al.* [9] also reported that there are two essential mechanisms for membrane fouling in the microfiltration process, namely pore fouling for the initial sharp drop and cake formation for long-term flux decline. Therefore, modelling of the fouling mechanisms in UF processes is significant.

Recent work on the modelling of the dead-end ultrafiltration of FAs, TGs and a mixture (TGs–FAs) employed the Hermia model. The fouling mechanisms were predicted by the incorporation of four different mechanisms comprised of complete blocking, intermediate blocking, standard blocking and cake formation. However, the previous analysis clearly showed some discrepancies between the normalised flux data and these predictions using classical pore blockage, pore constriction and cake formation. The poor fitting was probably due to the proposed Hermia model since it contains only one experimentally or individually fitted parameter. In this case, it can be suggested that a fouling transition between pore blocking and cake formation takes place [10].

Therefore, a developed combined pore blockage and cake formation model was applied for fouling prediction which accounts for initial pore blockage and subsequent fouling due to cake formation over the blocked regions [11, 12]. The model was successfully applied during protein fouling [11], humic acid fouling [13-15], coconut milk [16] and polyethylene glycol (PEG) fouling [17]. Recently, Rezaei *et al.* [18] compared the application of classical models and combined models during the microfiltration of whey. They deliberately applied three combined models, namely complete blocking-cake formation, intermediate blocking-cake formation and standard blocking-cake formation, each of which include two-phases of combined blocking. Additionally, the filtration time and operating conditions are major factors that differentiate the classical and combined models.

Basically, according to the classical model, fouling behaviour can be predicted either by the pore model followed by cake formation or vice versa. However, for combined models, pore blocking is always the main mechanism followed by cake formation over the entire filtration time. Furthermore, a similar combined model was developed by Bolten *et al.* [19].

According to the model, cake formation and complete pore blocking occur concurrently by taking into account the blocked areas and resistance from the cake model. They believed that the rate of complete blocking was slow mainly due to the high resistance of cake formation. It

was suggested that a cake was consistently scattered over the blocked or unblocked membrane pores at the same rate. Therefore, the ability of the fluid to pass through the plugged pores would be reduced due to cake build-up over the surface which became thicker by the end of filtration.

Recently, Peng and Tremblay [20] applied the combined model proposed by Ho and Zydney [11] during the microfiltration of oily wastewaters. They found that the experimental data were in good agreement with the combined pore blockage and cake filtration model. The results were also modelled initially using four classical models and it was found that intermediate blocking dominated the initial flux decay before cake filtration. They proposed that pore blocking was due to the presence of oil, grease and colloids.

The aim of this paper is to verify the fouling mechanisms occur during the filtration solely from the experimental data. Combined Blocking Model was chosen to assess and validate the fouling mechanism during the removal of organic solutes (TGs as well as TGs–FA mixture) which synthesizing sweetwater solutions. Numerous studies which are discussed previously only concentrate to the evaluation of blocking model to organic matter, protein solutions, colloidal and particles, whereas less attention has been paid to the role of organic solutes in aqueous solution. Therefore, the potential of TG and long hydrocarbon chain oleic acid with limited solubility to the flux decline profile was analyzed when treating the glycerin-water mixture. The influence of membrane surface chemistry, solute-solute interaction (TG and FA) and solutions's pH to the flux decline and permeate flux was studied. The blocking mechanism was modeled using Combined Blocking Model and the predictions have been compared with experimental data.

2.0 COMBINED BLOCKING MODEL

In this study, the Combined Blocking Model developed by Ho & Zydney [11] is used to validate the blocking mechanism in the ultrafiltration of glycerin-rich solution.

According to Ho and Zydney [11], filtrate flux through a fouled membrane is equal to the sum of the flow rate through the open and blocked pores according to the following equation:

$$Q = Q_{open} + Q_{blocked} \quad (1)$$

Then, the equation was evaluated mathematically to yield an expression for the filtrate flux rate ($L/m^2.h$) through the fouled membrane at any given filtration time (min) as:

$$\frac{J}{J_o} = \exp(-kt) + \frac{R_m}{R_m + R_c}[1 - \exp(-kt)] \quad (2)$$

where R_m, R_c and k are hydraulic membrane resistance (m^{-1}), the resistance of the solute cake that forms over the membrane surface (m^{-1}) and the combined model fitted parameter (h^{-1}), respectively.

3.0 EXPERIMENTAL

3.1 Chemicals

The high purity glycerin (USP) used to prepare the feed solution was supplied by Sigma Aldrich. Its molecular weight was 92.09 g/mol. The commercial triglycerides (RBD Palm Olein, 870 g/mol) were obtained from the local hypermarket. The analytical grade oleic acid (282.46 g/mol) was purchased from Merck and used as received. It was used as a co-foulant model in the feed solution for

determination of flux decline in glycerin-water solutions.

3.2 Preparation of Glycerin-water Solutions with TG and TG-FA.

The feed solution was prepared by adding 1% (v/v) TG into 15% (v/v) glycerine and the rest is pure water, while the oleic acid was added into the mixtures based on its maximum solubility (0.003 g/L in pure water). Prior to combination with glycerine, the TG was initially added in 84% (v/v) ultra-pure water and stirred for 40 minutes to minimize heterogeneity effects. Initially, the pH of the feed solution was ranging between pH 4.5-4.8 and varied to pH 3 and pH 10 with the addition of several drops of hydrochloric acid and sodium hydroxide. It was measured with a pH meter (Mettler Toledo). The selection of the pH range was based on the effect of pH values during the ultrafiltration of FA and TG as reported in the literature studies [21, 22]. The size of oil droplet distributions for the prepared solution was determined using particle analyzer (Mastersizer Malvern).

3.3 Membrane

A circular flat sheet PES membrane (SelRo MPF-U20-P) and PVDF membrane (GE Osmonic) were purchased from Sterlitech Corporation is used in the flux decline experiments. The properties of the membranes exhibited in Table 1. Both membranes were of the composite type using proprietary material was not disclosed by the manufacturer. New membranes were soaked in pure water overnight prior to each run in order to remove the preservative liquids from the manufacturer before it can be used.

3.4 Flux Decline Experiment

Experiments were performed in the dead-end ultrafiltration stirred cell (Sterlitech) as described elsewhere [23]. Then, the permeability of PES and PVDF membranes was determined using pure water at different pressures (2-5 bar). The temperature was set constantly at 40^{o}C as this was the minimum temperature applied in oleochemical industry to carry out the hydrolysis. It was selected to perform the flux decline experiments by placing the whole set in the water bath at the set temperature. Then, both the stirred cell and solution reservoir were charged with the prepared mixtures to study the effects of membrane and solution chemistry on flux decline. The pressure applied for the fouling experiments is constantly at ΔP=2 bar. The volume of permeate samples was collected within 60 minutes. The flux was normalized with respect to the pure water flux through fresh membrane as described elsewhere [24]. After the fouling experiments have been completed, the membrane was rinsed with pure water twice for 30 seconds. Pure water flux was measured before and after filtration to ensure whether the membrane could be used for the next analysis after cleaning.

4.0 RESULTS AND DISCUSSION

4.1 Membrane Surface Chemistry

Figure 1 shows the fitting of the experimental results and the combined model prediction for the PES25 and PVDF membranes after the ultrafiltration of TG. It is visible that the combined model fits the experimental data well for both membrane materials. This may be due to the quick adsorption of TG at the beginning of filtration process which

results in a rapid flux decline. Then, the flux decline further and almost reaches a steady state at later times due to cake formation. A similar result has been reported by Wang *et al.* [25].

Table 1 Membrane Properties

Membrane	Material	MWCO (Da)	Contact angle, θ	r_p (nm)
PES 25	Polyethersulphone	25000	74.10	3.13
PVDF	Polyvinylidenefluoride	30000	72.60	3.32

On the other hand, it is interesting to note that the PES25 membrane suffered more severe flux decline than the PVDF membrane. According to the analysis, the kinetic fouling constant for PES25 membrane was 0.3636 min^{-1}, which is significantly higher than that of the PVDF membrane (0.1830 min^{-1}). These values were obtained from the fitting analysis of Equation 2 which is done by using SigmaPlot. It shows that the fouling rate of the PES membrane occurred drastically once filtration started. This finding suggests that the hydrophobic behaviour of the PES25 membrane and TG might enhance solute–membrane interactions and accelerate solute adsorption to the pore wall. Consequently, the PES25 membrane underwent more severe normalised flux reduction than the PVDF membrane.

Additionally, the model prediction correlates well with the normalised flux as presented in Table 2. The comparison was made with the data fitting with Hermia model as reported previously [26]. It can be said that the higher R^2 and the lower *S.D.*(%) correspond to a better fit of the model, and the analysis supports the fitting as depicted in Figure 1. It is interesting to note that the fitted R^2 for the combined model is considerably higher than the single model (Hermia model); this is valid for the PES25 and PVDF membranes. It suggests that the fouling mechanism is mainly driven by pore blockage and cake formation. Furthermore, the combined model depicts a smaller *S.D.*(%) than the Hermia model, showing that the model can predict flux decline behaviour during the ultrafiltration of glycerine–water solutions plus TG.

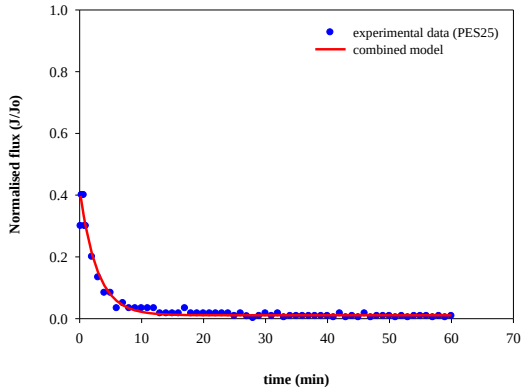

(a)

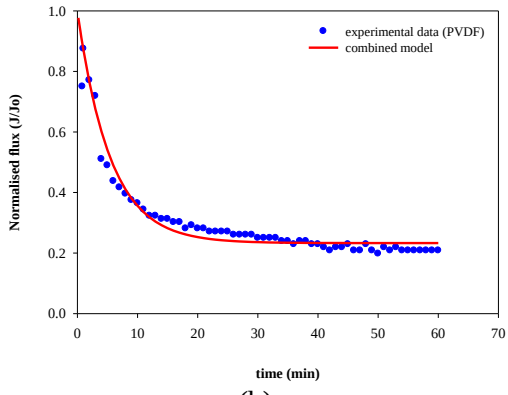

(b)

Figure 1 Normalized flux decline of TG predicted by combined blocking model, (a) PES25 and (b) PVDF membrane

4.2 Influence of Different Solutes: FA, TG and Combination of TG–FA

The type of foulant plays an important role in inducing flux decline and membrane fouling. Figure 2 illustrates

Table 2 Comparison of R^2 values and *S.D.* (%) between Hermia and combined models for different membrane materials

TG	R^2		*S.D.(%)*	
	Hermia model	combined model	Hermia model	combined model
PES25	0.9489	0.9687	27.22	13.45
PVDF	0.8678	0.9541	13.97	11.69

the fitting of the combined pore blockage–cake formation model to the normalised flux profiles of membranes fouled by a mixture of three different foulants: glycerine–water plus FA, TG and TG–FA mixtures. It is clearly shown in Figures 2(a) and (b) that the effect of TG on flux profiles is most significant compared to the membrane fouled by a mixture of TG–FA and FA alone. As observed in both figures, rapid flux decline occurred during initial ultrafiltration (*t<10 min*) for the PES25 membrane, possibly due to the deposition of oil droplets onto the membrane surface and inner pore walls, which led to the clogging of pores [27].

Further, some of the large oil droplets took part in the formation of a gel layer during the initial stage, and hence accelerated drastic flux decline. Therefore, at later time points, the final normalised flux almost reached a steady state value, suggesting that the formation of the cake layer was responsible for the fouling extension and reduced the pore blocking resistance. This hypothesis is consistent with other research conducted during the microfiltration of whey [15]. This phenomenon implies that during long term operation, the membrane surface area was entirely covered with a gel layer. Therefore, this might prevent the membrane pores from being blocked further.

On the other hand, the influence of FA is insignificant compared to the influence of TG. The sequences of severity follow this order: glycerine–water solutions (plus FA) < (plus TG–FA mixture) < (plus TG). This finding suggests that the MW of FA is much smaller than the MW of TG, so the solution plus FA suffers less fouling compared to the solution plus TG. Moreover, the combined pore blockage–cake formation model reveals considerably good fitting with the experimental results.

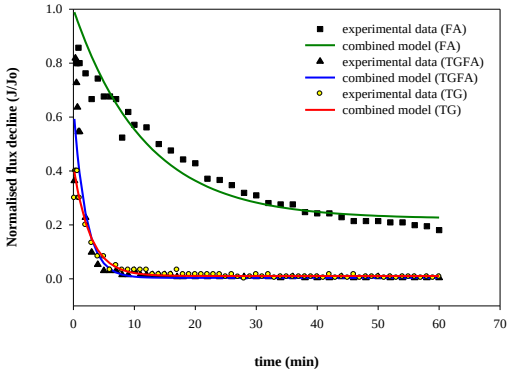

(a)

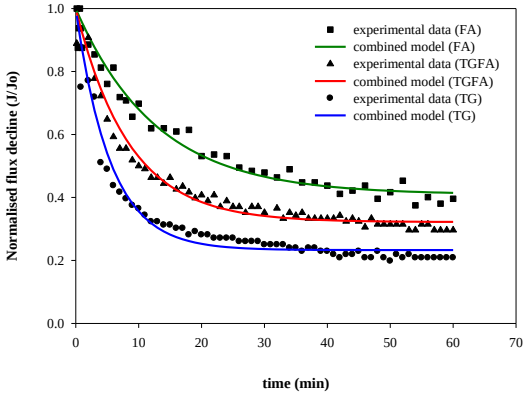

(b)

Figure 2 Normalized flux decline of different mixtures predicted by the combined blocking model, (a) PES25 and (b) PVDF membrane

Table 3 Comparison of R^2 and *S.D%* values between the Hermia and combined models for different foulants

R^2	PES25		PVDF	
	Hermia	combined	Hermia	combined
FA	0.9604	0.8218	0.9639	0.9698
TG–FA	0.8847	0.9023	0.8679	0.949
TG	0.8608	0.9687	0.8678	0.9541
S.D.(%)	PES25		PVDF	
	Hermia	combined	Hermia	combined
FA	5.5	21.63	3.5	5.33
TG–FA	46.51	39.36	14.86	6.62
TG	39.72	94.25	19.02	11.69

Evidently, the results of high correlation coefficients (R^2) as depicted in Table 3 indicate an excellent fit with combined model compared to the single model. These correlations corroborate the fittings illustrated in Figure 2. As can be seen in Table 3, the combined model reveals $R^2 > 0.9$ for all types of foulants except for FA (R^2 0.8218), and this range is valid for both membrane materials if compared to Hermia model ($R^2 < 0.9$).

According to Peng and Tremblay [12], the best fit with the combined model incorporates a two−parameters model, while the Hermia models are single−parameter models. Therefore, it is possible to predict a fouling mechanism which can be divided into two stages, a sharp decline and a pseudo−steady stage [8]. Nevertheless, the Hermia model also presents a noticeably good correlation for FA with $R^2 > 0.9$. This is probably due to the fact that the normalised flux profiles of FA continuously decrease and very slowly achieve a steady−state condition, which perhaps can be maintained over very long time scales. As a matter of fact, the fouling mechanism occurs simultaneously within a filtration time which could not predicted by using the Hermia model [28]. Conversely, the Hermia model gives a poor correlation for the PES25 and PVDF membranes for both TG and the TG–FA mixtures with $R^2 <$ 0.9. This suggests that the PES25 and PVDF membranes suffer drastic flux decay over a short period of time (within the first 10 min) and are almost maintained in a steady state as the filtration time.

A similar trend was observed for *S.D.(%)* as shown in Table 3. The combined model gives larger variations with the experimental data for the glycerine−water solutions plus FA. This observation is based on the higher *S.D.(%)* values compared to the Hermia model. This indicates that the flux profile of low MW FA gradually decreased and required a very long operation time to achieve a pseudo−steady state. Hence, the combine model fit the experimental data of FA less well. Conversely, the combined model gives the least *S.D.(%)* for TG and the TG–FA mixture, suggesting that the model predict the flux profile quite well. This is mainly attributed to the occurrence of severe pore blockage over shorter periods of time and subsequent fouling

due to the formation of a gel layer over the initially blocked areas.

4.3 Influence of Feed Characteristics

Figure 3 shows the fitting of the experimental data with the combined pore blockage–cake formation model for different feed characteristics. It can be clearly observed that the suggested model provides better agreement with the experimental data as expected at low and high pH.

It can be conjectured that the feed pH has a significant effect on the fouling mechanism during the ultrafiltration of a glycerine–water solutions plus FA, TG–FA mixture or TG. The results indicate a rapid decay in the flux profile at < 10 min, apparently due to the drastic clogging of membrane pores. Further, as the filtration time increased, the normalised fluxes nearly attained a steady state, suggesting the formation of a fouling layer on the surface. This observation implies that cake formation was dominating the fouling mechanism for the TG–FA mixture as well as TG in both feed characteristics. A similar trend was reported by Chang *et al*. [29] in their study on the nanofiltration of natural organic matter (NOM).

The fitness coefficients as reported in Table 4 was associated with the fitting as depicted in Figure 3. It is noteworthy that the fitness coefficients of the combined model for the PES25 membrane reveal $R^2 > 0.9$ at low pH (pH 3) and high pH (pH 10). Nevertheless, the R^2 values for FA in the acidic and basic solutions were lower than 0.85 and 0.76, respectively, suggesting a large discrepancy between the experimental data and the combined model. This finding explains why the normalised flux of FA declined incessantly within the filtration time and slowed to achieve a stable flux, which would probably occur over a prolonged operation time. This suggests that membrane fouling did not exhibit a two-step process under these conditions. At low pH, the FA was greatly undissociated and was allowed to adsorb within the membrane pores. According to the literature, this mechanism might slow down, but persists for a long time [28]. On the other hand, with a high pH feed solution, FA have the tendency to fully dissociate and behave as an anionic surfactant (Fereidoon 2005) which might induce negative charges on the hydrophobic membrane [2, 30].

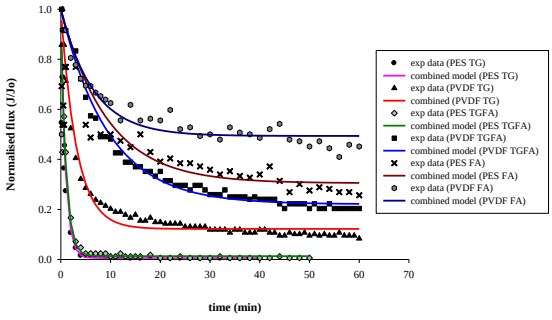

(a)

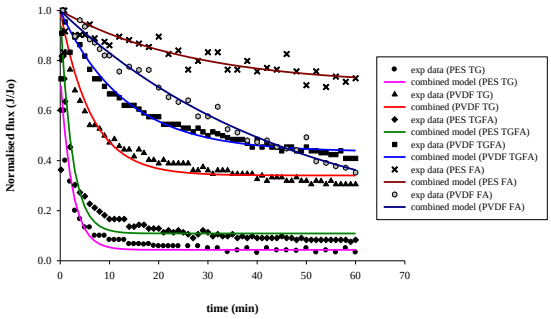

(b)

Figure 3 Influence of feed characteristics on normalised flux decline for different mixtures predicted by the combined blocking model: (a) acidic solution and (b) alkaline solution

The effect of this characteristic, coupled with the repulsive interaction between the FA and the hydrophobic membrane, was substantial enough to release the fouling layer and transfer

Table 4 Comparison of R^2 values between the Hermia and combined models for different feed characteristics (PES25 and PVDF membrane)

R^2	Acidic (PES25)		Acidic (PVDF)	
	Hermia	combined	Hermia	combined
FA	0.8666	0.8141	0.9686	0.9411
TG–FA	0.8808	0.9106	0.9788	0.9332
TG	0.8489	0.9634	0.9568	0.9551
R^2	Alkaline (PES25)		Alkaline (PVDF)	
	Hermia	combined	Hermia	combined
FA	0.8122	0.7475	0.9455	0.9638
TG–FA	0.9752	0.9743	0.9758	0.9815
TG	0.7896	0.9603	0.9468	0.9681

the FA from the membrane surface to the permeate side. This hypothesis was also supported by Ang *et al*. [31] in their fouling study on organic foulants from wastewater effluents. Therefore, the formation of a fouling layer was diminished and the normalised flux tended to decline continuously. Consequently, the combined model could not predict the normalised flux decline of FA using the PES25 membrane.

On the other hand, the PVDF membrane was found to have $R^2 > 0.9$ with both feed characteristics, which indicates an excellent fit with the experimental data and corroborates this mechanism. This good fit suggests that pore blockage and the growth of a gel layer were responsible for membrane fouling and probably occurred simultaneously during the filtration process.

5.0 FITTING PARAMETERS AND FOULING PROPENSITY CORRELATION

The purpose of this modelling was to substantiate data fitting. However, apart from that, it is interesting to observe that the fitting parameters manifested a reasonable consistency. Figure 4 shows the correlation between the fouling constant, k (min^{-1}) and the type of foulant. The fitting parameter for the PES25 membrane was considerably larger and can be ascribed to greater fouling severity than the PVDF membrane. The kinetic fouling constant trends indicate that electrostatic interactions near the membrane surface accelerated foulant adsorption once filtration began and therefore had a greater impact on membrane fouling.

Moreover, it should be noted the fouling constants were affected by the foulants. The foulants were categorised based on the molecular weight (MW) and approximate size of the solute in the feed solution. According to Figure 5, the size of the solute increased as follows: *FA* (3.56 µm) < *TG–FA* (44.74 µm) < *TG* (63.25 µm). It can be conjectured that the size distribution would be increased as the MW of the solutes increased. Nevertheless, as discussed previously, the size of the TG–FA droplets was smaller than TG droplets, mainly due to the diffusivity effect which took place in the feed solution. The ability of small FA to diffuse in the feed might diminish the aggregation of TG and yet reduce droplet size. Therefore, it was observed that the k value significantly increased

from 0.085 to 0.495 min^{-1}, and from 0.078 to 0.183 min^{-1} for the PES25 and PVDF membranes, respectively. This suggests that convection aids in rapidly carrying the small FA droplets into the pores and may cause preferential adsorption within the pores compared to large solutes like TG and the TG–FA mixture. Thus, a small and flexible solute like FA would be expected to cause more severe, prolonged normalised flux decline compared to the large size and long hydrocarbon chain of a solute like TG. Therefore, it would be expected to cause a greater resistance to flow through the membrane [18].

This hypothesis is associated with the ratio of hydraulic resistance over the specific gel resistance (R_m/R_g) as shown in Figure 6. It is clearly illustrated that the R_m/R_g for the glycerine–water solutions plus FA was considerably higher compared to the other solutes; this was reported to be 0.287 for PES25 and 0.692 for PVDF. It is conjectured that small FA are able to be compressed more easily than TG which increases the packing density. Consequently, the hydraulic resistance over the specific gel becomes higher and the permeability would be expected to decline. Additionally, according to the highest *k* value, this indicates that TG underwent severe fouling probably due to drastic and greater adsorption within the pores once UF was initiated. Since TG possess long hydrocarbon chains in their molecular structure, it may be speculated that TG might be more difficult to compress than small FA. The tendency of TG to lie horizontally over the membrane surface results in preferential gel formation near the membrane pores. Therefore, this formation is believed to cause greater specific gel resistance and reduce the ratio of R_m over R_g for flow through UF, which was reported to be 0.006 for PES25 and 0.304 for PVDF, respectively.

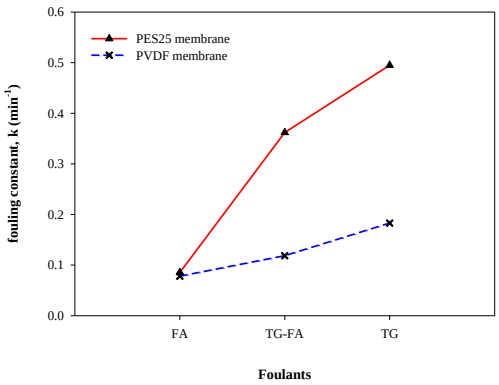

Figure 4 Correlation between *k* and foulants for the PES25 and PVDF membranes

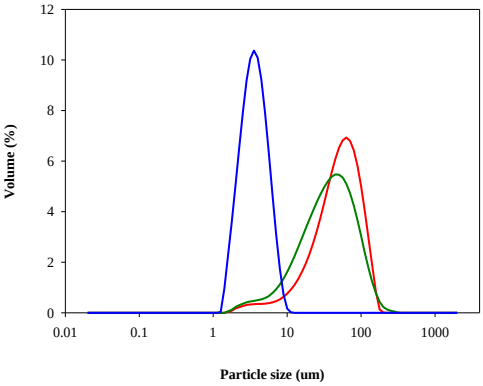

Figure 5 Distribution of solutes in glycerine–water solutions

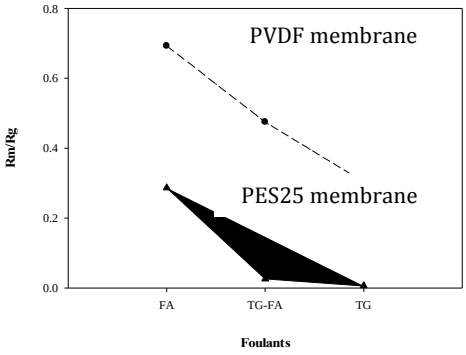

Figure 6 Ratio of hydraulic over specific gel resistance for the PES25 and PVDF membranes

Figure 7 depicts the correlation between the fouling parameter, *k* (min^{-1}) and feed characteristics during the

ultrafiltration of FA, TG–FA and TG. As seen in Figure 7, both the PES25 and PVDF membranes demonstrated a higher fouling constant at low pH and a lower *k* at high pH, suggesting that both membranes experienced severe fouling in the acidic feed solution. The values of *k* for the PES25 membrane were reported to be between 0.107 to 1.089 min^{-1} in an acidic solution and were significantly reduced to the range of 0.037–0.426 min^{-1} in a basic solution. In contrast, for the PVDF membrane, the fouling parameters are comparatively lower than for the PES25 membrane, which implies that the PVDF membrane endured less fouling compared to the PES25 membrane. As illustrated in Figure 7, the *k* values for PVDF in an acidic solution ranged from 0.105 to 0.316 min^{-1}, and the values were reduced to 0.021–0.159 min^{-1} in a basic solution. Under acidic conditions, FA was less dissociated, whereas the oil droplets behaved as a hydrophobic foulant. This induced a weak electrostatic repulsive between the foulants in solution and the less negatively charged membrane surface as well as the pre–formed fouling layer. This hypothesis was reported by Sutzkover-Gutman *et al*. in their fouling study with humic substances [32]. Therefore, intensified fouling occurs, probably due to major deposition within pores and the formation of a fouling layer near the pore entrance.

Figure 8 illustrates the ratio of R_m/R_g for the two membranes with different feed characteristics. The trend was opposite from the fouling parameters as depicted in Figure 7. The ratio for the two membranes was higher at high pH, which indicates that the alteration in feed characteristics to an alkaline condition might diminish

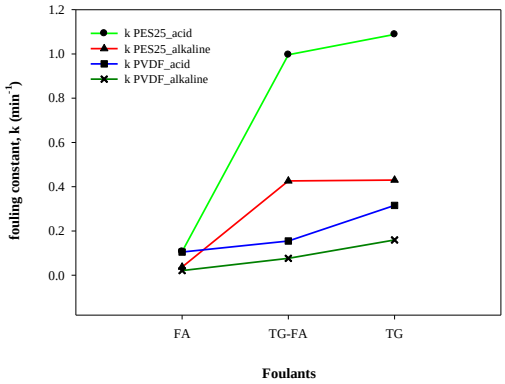

Figure 7 Correlation between *k* and pH for the PES25 and PVDF membranes

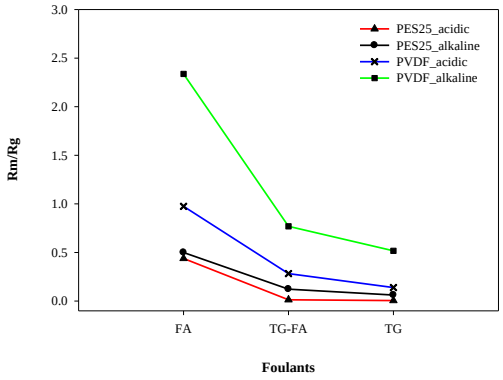

Figure 8 Ratio of hydraulic over specific gel resistance for the PES25 and PVDF

the formation of a gel layer and weaken the adherence of small FA and oil droplets to the pore wall. The addition of NaOH to the feed solution probably deteriorates the van der Waals interactions among the molecules and reduces their ability to aggregate. Therefore, the small solutes were easily moved to the permeate side and reduces the formation of an oil layer. As a result, the specific gel resistance is decreased and permeation improves. On the other hand, the two membranes showed a low R_m/R_g at low pH. This assumes that the addition of HCl induces the aggregation of oil droplets and the formation of coalescences. This might accelerate the build-up of oil droplets within the pores and membrane surface and result in the formation of a gel layer.

Consequently, this phenomenon increases the specific cake resistance and enhances the resistance to permeation through the membrane.

6.0 CONCLUSIONS

The ultrafiltration of glycerine–water solutions containing FA, TG and TG–FA mixtures results in a drastic fall in flux over time which occurs severely in the initial stages of filtration membrane at different pH. The influences of membrane surface and feed chemistry as well as solute-solute interactions have been studied. The prediction of fouling propensity was using Combined Blocking Model and being compared with modified Hermia model with a single parameter. As a conclusion, there are pore blocking model fit well to the experimental data and some did not due to large deviation between experiment and the model. It is observed that different blocking mechanisms may take place during the ultrafiltration process which leads the combination of two or more in the process. In the case of different membrane materials (PES25 and PVDF membranes), two stages of the fouling mechanism seem to obviously occur, which could be an initial phase of some type of pore blocking followed by cake formation. The Combined Blocking Model gives significantly good correlation to PES membrane with R^2 more than 0.96. The trend is similar for PVDF membrane. The two membranes represent higher *S.D.(%)* with blocking models at 27.22 and 13.97%, respectively, showing that the Hermia model did not fit well the experimental data. Nevertheless, in the case of different solutes, the fouling behaviour of TGs and TG-FA mixtures was successfully predicted by the combined blocking model. The least *S.D. (%)* about 11.69 and 6.62% for TGs and TG-FA, respectively, indicates that pore blocking followed by cake formation at long operation time would gave the best prediction of behaviour. Nevertheless, the combined model gave the poor fitting to the flux profile of small FA under all conditions due to the large variation between the experimental data and the model (with R^2 0.8218 and *S.D.(%)* 21.63%) . This phenomenon could be explained by the ability of small FA to enter the membrane pores more easily than TG and implied the occurrence of pore blocking within the filtration time. Hence, the fluxes tended to decline continuously and approached a steady–state value with prolonged operation times, leading to the worst fitting with the combined model. Furthermore, the blocking prediction using this combined blocking model was good enough for both membranes in acidic as well as basic pH solution, respectively. The highest R^2 values *(> 0.9)* are consistent with the fitting. As a matter of fact, the combined blocking model in a good agreement with the normalised flux decline of the PVDF membrane in both feed solutions. The minimum deviation between experimental data and prediction confirms that the oily layer from TGs and FA deposited on the membrane surface at all pH values.

ACKNOWLEDGEMENT

The authors wish to express their gratitude to the KLK Oleochemical Sdn. Bhd, Kundang Industrial Estate for supplying the sweetwater and glycerin samples to conduct this study. The authors also wish to gratefully acknowledge the financial support for this work by Ministry of Science and Technology (ScienceFund) through the project no. 02-01-02-SF0529 and

would like to thank Environmental Laboratory (UniKL MICET) for the particle size analyzer (MALVERN).

REFERENCES

[1] M. C. Burshe, S. B. Sawant, V. G. Pangarkar. 1999. Dehydration of Glycerin-water mixtures by Pervaporation. *JAOCS.* 76: 209-214.

[2] S. Fereidoon. 2005. Bailey's Industrial Oil and Fat Products: Sixth Edition Vol. 1 Edible Oil and Fat Products: Chemistry, Properties, and Health Effects. United States: A John Wiley & Sons, Inc., Publication.

[3] D. B. Khairnar, V. G. Pangarkar. 2004. Dehydration of Glycerin/water Mixtures by Pervaporation using Homo and Copolymer Membranes. *JAOCS.* 81: 505-510.

[4] L. Jeromin, W. Johannisbauer, S. Blum, R. Sedelies, H. Moormann, B. Holfoth, J. Plachenka. 1996. Process for the Purification of Glycerol Water. U.S.Patent 5,527,974.

[5] A. W. Mohammad, P. T. Yap, T. Y. Wu. 2009. Performance of Hydrophobic Ultrafiltration Membranes in the Treatment and Protein Recovery From Palm Oil Mill Effluent (POME). *Des. Water Treatment.* 10: 332-338.

[6] T. Y. Wu, A. W. Mohammad, J. M., Jahim, N. Anuar. 2007. Palm Oil Mill Effluent (POME) Treatment and Bioresources Recovery Using Ultrafiltration Membrane: Effect of Pressure on Membrane Fouling. *Biochemical Eng. Journal*. 35: 309-317.

[7] W. J. Zhang, M. Zhang, F. Xiao, L. P. Fang, D. S. Wang. 2014. Pretreatment of High Strength Waste Emulsions by Combined Vibratory Shear Enhanced Process with Fenton Oxidation. *International Journal of Env. Sci. and Techn.* 11: 731-738.

[8] A. Salahi, M. Abbasi, T. Mohammadi, T. 2010. Permeate Flux Decline during UF of Oily Wastewater: Experimental and Modeling. *Desalination.* 251: 153-160.

[9] Y. Pan, W. Wang, T. Wang, P. Yao. 2007. Fabrication of Carbon Membrane and Microfiltration of Oil-in-Water Emulsion: An Investigation on Fouling Mechanisms. *Sep. and Purif. Techn.* 57: 388-393.

[10] S. Kosvintsev, R. G. Holdich, I. W. Cumming, V. M. Starov. 2002. Modelling of Dead-end Microfiltration with Pore Blocking and Cake Formation. *J. Memb. Sci.* 208: 181-192.

[11] C.-C. Ho, A.L. Zydney. 2000. A Combined Pore Blockage and Cake Filtration Model for Protein Fouling During Microfiltration. *J. Colloid and Interface Sci*. 232: 389-399.

[12] H. Peng, A. Y. Tremblay. 2008. Membrane Regeneration and Filtration Modeling in Treating Oily Wastewaters. *J. Memb. Sci.* 324: 59-66.

[13] W. Yuan, A. Kocic, A. L. Zydney. 2002. Analysis of Humic Acid Fouling During Microfiltration Using a Pore Blockage-Cake Filtration Model. *J. Memb. Sci*. 198: 51-62.

[14] H-C, Kim, B. A. Dempsey. 2013. Membrane Fouling due to Alginate, SMP, EfOM, Humic Acid, and NOM. *J. Memb. Sci*. 428: 190-7.

[15] C. Y. Tang, Q. She, W. C. L. Lay. R. Wang, A. G. Fane. 2010. Coupled Effects of Internal Concentration Polarization and Fouling on Flux Behavior of

Forward Osmosis Membranes During Humic Acid Filtration. *J. Memb. Sci*. 354: 123-33.

[16] C. Y. Ng, A. W. Mohammad, L. Y. Ng, J. M Jahim. 2014. Membrane Fouling Mechanisms during Ultrafiltration of Skimmed Coconut Milk. *J. Food Eng.* 142: 190-200.

[17] M. C. V. Vela, S.A. Blanco, J. L. García, E. B. Rodríguez. 2006. Application of a Dynamic Model that Combines Pore Blocking and Cake Formation in Crossflow Ultrafiltration. *Desalination.* 200: 138-139.

[18] H. Rezaei, F.Z. Ashtiani, A. Fouladitajar. 2011. Effects of Operating Parameters on Fouling Mechanism and Membrane Flux in Cross-flow Microfiltration of Whey. *Desalination*. 274: 262-271.

[19] G. Bolten, D. LaCasse, R. Kuriyel. 2006. Combined Models of Membrane Fouling: Development and Application to Microfiltration and Ultrafiltration of Biological Fluids. *J. Membr. Sci*. 277: 75-84.

[20] H. Peng, A. Y. Tremblay. 2008. The Selective Removal of Oil from Wastewaters While Minimizing Concentrate Production using a Membrane Cascade. *Desalination.* 229: 318-330.

[21] K. L. Jones, C. R. O' Melia. 2001. Ultrafiltration of Protein and Humic Substances: Effect of Solution Chemistry on Fouling and Flux Decline. *J. Membr. Sci*. 193: 163-173.

[22] A. Lobo, A. Cambiella, J. M. Benito, C. Pazos, J. Coca. 2006. Ultrafiltration of Oil-in-Water Emulsions with Ceramic Membranes: Influence of pH and Crossflow Velocity. *J. Membr. Sci*. 278: 328-334.

[23] I. N. H. M. Amin, A. W. Mohammad, M. Markom, C. P. Leo, N. Hilal. 2010. Flux Decline Study during Ultrafiltration of Glycerin-Rich Fatty Acid Solutions. *J. Membr. Sci*. 351: 75-86.

[24] I. N. H. M. Amin, A. W. Mohammad, M. Markom, C. P. Le. 2010. Effects of Palm Oil-Based Fatty Acids on Fouling of Ultrafiltration Membranes during the Clarification of Glycerin-Rich Solution. *J. Food Eng.* 101: 264-272.

[25] Z. Wang, J. Chu, X. Zhang, X. 2007. Study of a Cake Model during Stirred Dead-End Microfiltration. *Desalination.* 217: 127-138.

[26] M. A. Indok Nurul Hasyimah, A. W. Mohammad. 2014. Assessment of Fouling Mechanisms in Treating Organic Solutes Synthesizing Glycerin-Water Solutions by Modified Hermia Model. *Ind. Eng. Chem. Res.* 53: 15213-15221. DOI:10.1021/ie502509d.

[27] Amin, I. N. H. M., Mohammad, A. W. & Hilal, N. 2014. Description of Membrane Fouling Characteristics during Uktrafiltration of Organic Foulants Contained In Sweetwater Solutions. *J. Env. Chem. Eng.* 2: 1243-1251.

[28] K. Katsoufidou, S. G. Yiantsios, A. J. Karabelas. 2005. A Study of Ultrafiltration Membrane Fouling by Humic Acids and Flux Recovery by Backwashing: Experiments and Modelling. *J. Membr. Sci.* 266: 40-50.

[29] E.-E. Chang, S.-Y. Yang, C.-P. Huang, C.-H. Liang, P.-C. Chiang. 2011. Assessing the Fouling Mechanisms of High-Pressure Nanofiltration Membrane Using the Modified

Hermia Model and the Resistance-in-Series Model. *Sep. Purif. Techn*. 79: 329-336.

[30] V. Chen, A. G. Fane, C. J. D. Fell. 1992. The Use of Anionic Surfactants for Reducing Fouling of Ultrafiltration Membranes: Their Effects and Optimization. *J. Membr. Sci*. 67: 249-261.

[31] W. S. Ang, A. Tiraferri, K. L. Chen, M. Elimelech. 2011. Fouling and Cleaning of RO Membranes Fouled by Mixtures of Organic Foulants Simulating Wastewater Effluent. *J. Membr. Sci*. 376: 196-206.

[32] I. Sutzkover-Gutman, D. Hasson, R. Semiat. 2010. Humic Substances Fouling in Ultrafiltration Processess. *Desalination*. 261: 218-231.